Supplementary Information

Smartphone-based fluoride-specific sensor for rapid and affordable colorimetric detection and precise quantification at sub-ppm levels for field applications

*Sritama Mukherjee,[†‡] Manav Shah,[†] Kamalesh Chaudhari,[†] Arijit Jana,[†] Chennu Sudhakar,[†] Pillalamarri Srikrishnarka,[†] Md Rabiul Islam,[†] Ligy Philip[‡] and Thalappil Pradeep[†]**

[†] DST Unit of Nanoscience (DST UNS) and Thematic Unit of Excellence (TUE), Department of Chemistry, Indian Institute of Technology Madras, Chennai 600036, India.

[‡] EWRE Division, Department of Civil Engineering, Indian Institute of Technology Madras, Chennai 600036, India.

*Corresponding author

E-mail: pradeep@iitm.ac.in

SUPPORTING INFORMATION CONTENT

Total number of pages: 13

Total number of figures: 11

TABLE OF CONTENTS

Supplementary information 1

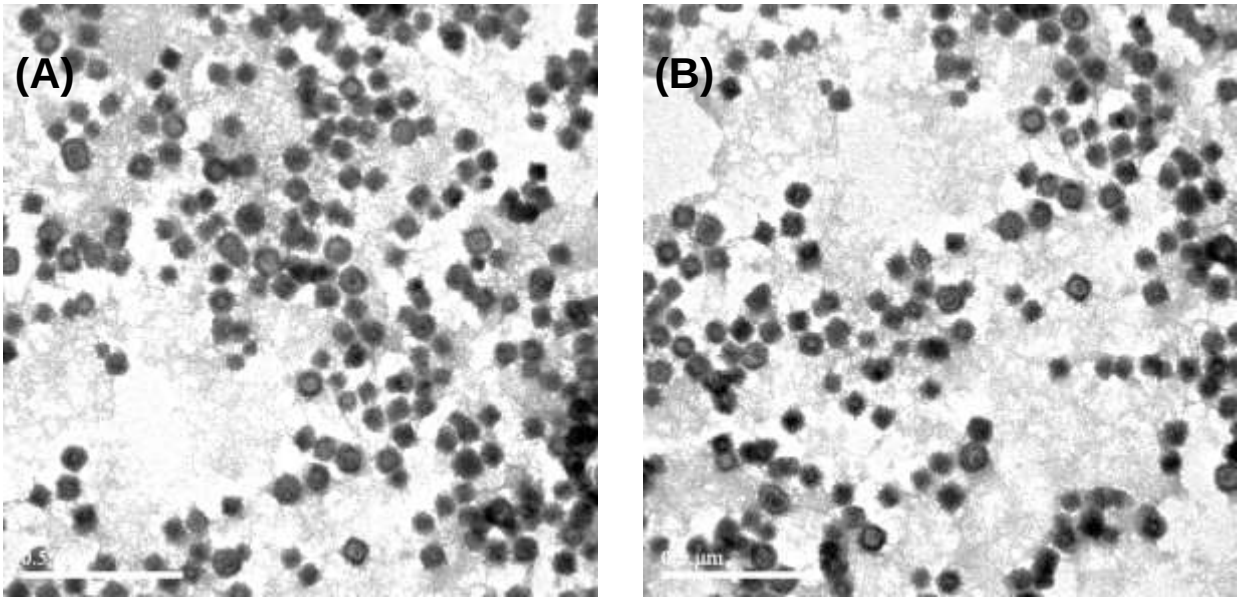

Figure S1. (A) and (B) show large area TEM images showing the structure of ceria@zirconia nanocages.

Supplementary information 2

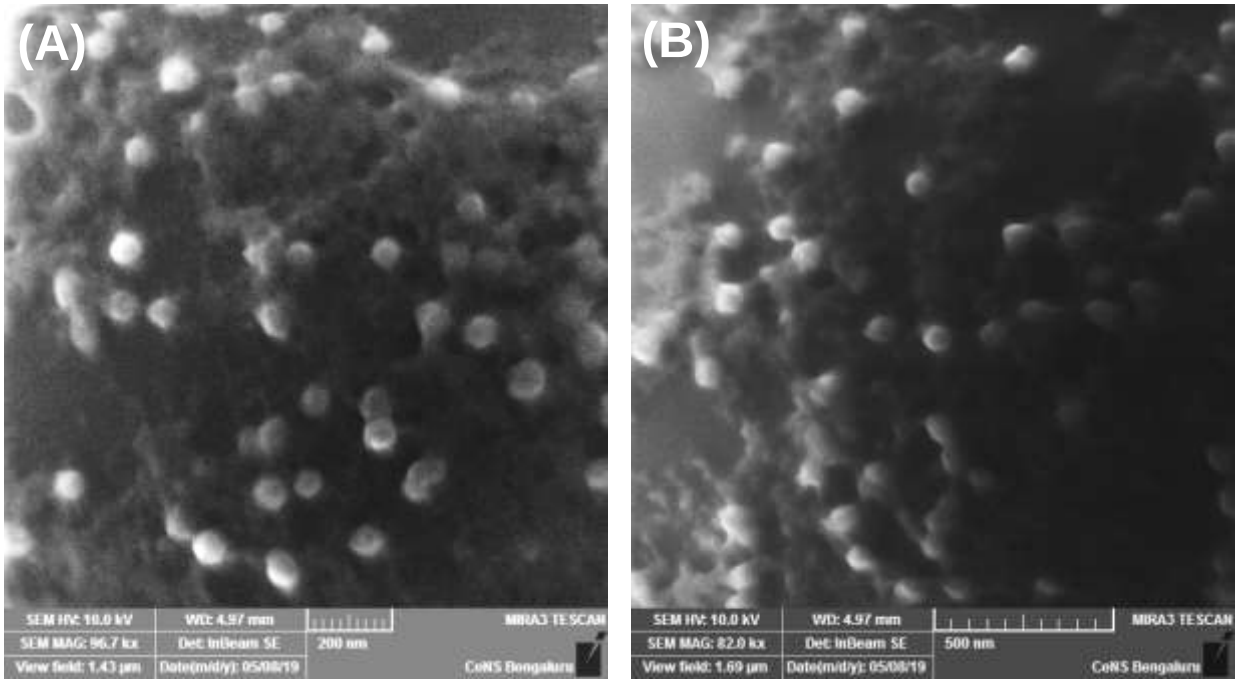

Figure S2. (A) and (B) show large area FESEM images for ceria@zirconia nanocages showing their near cubic shapes.

Supplementary information 3

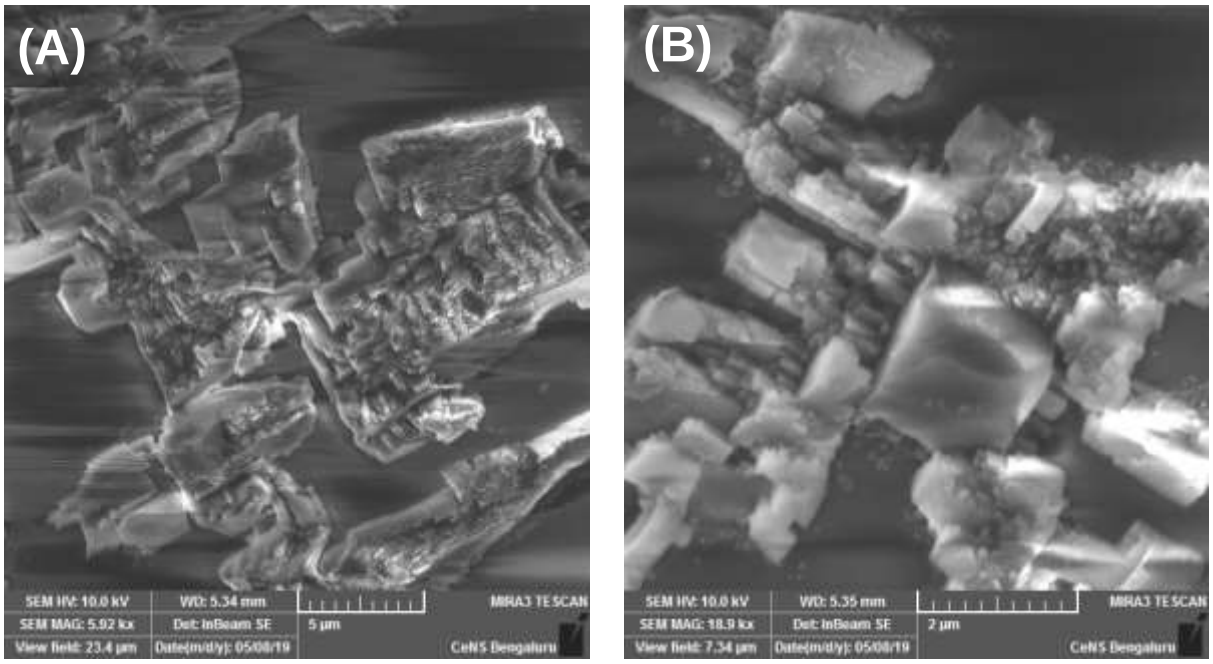

Figure S3. (A) and (B) show large area FESEM images of ceria@zirconia nanocages after their interaction with F^- ions.

The images show the aggregation of fluoride around the nanocages upon interacting with F^- in water.

Supplementary information 4

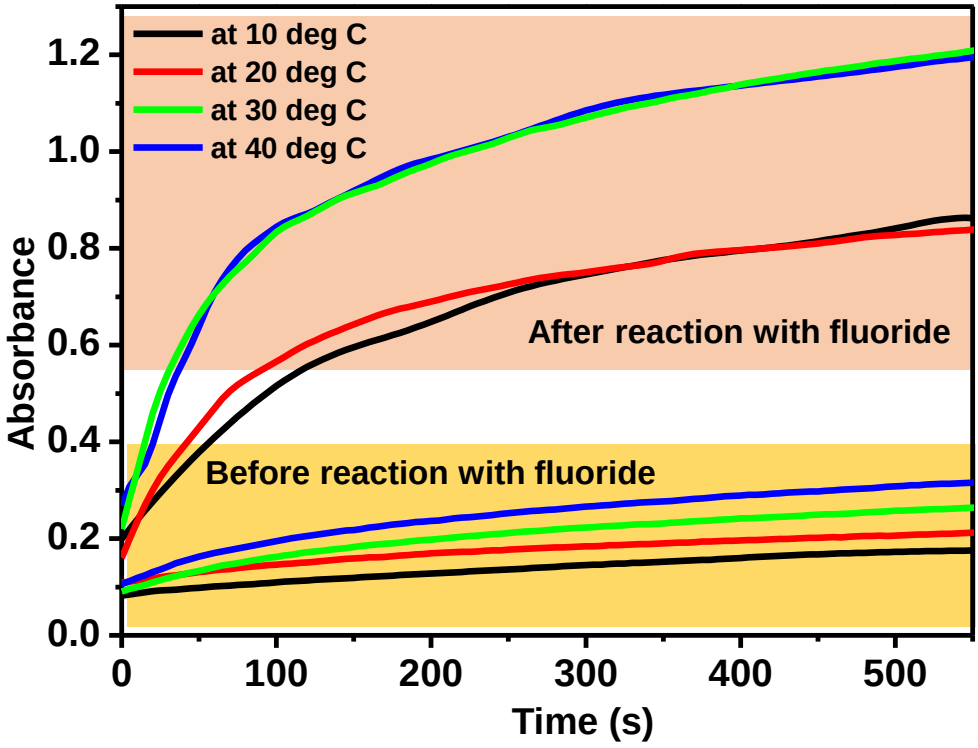

Figure S4. Temperature dependent kinetics of NC-XO before and after interaction with F^- ions.

The UV-vis spectra shows the NC-XO absorbance with and without F^- at 10, 20, 30 and 40°C. It is clear that higher temperature facilitates the reaction responsible for color change, thus rate of reaction increases. The kinetics of fluoridated samples show much higher increase then control samples.

Supplementary information 5

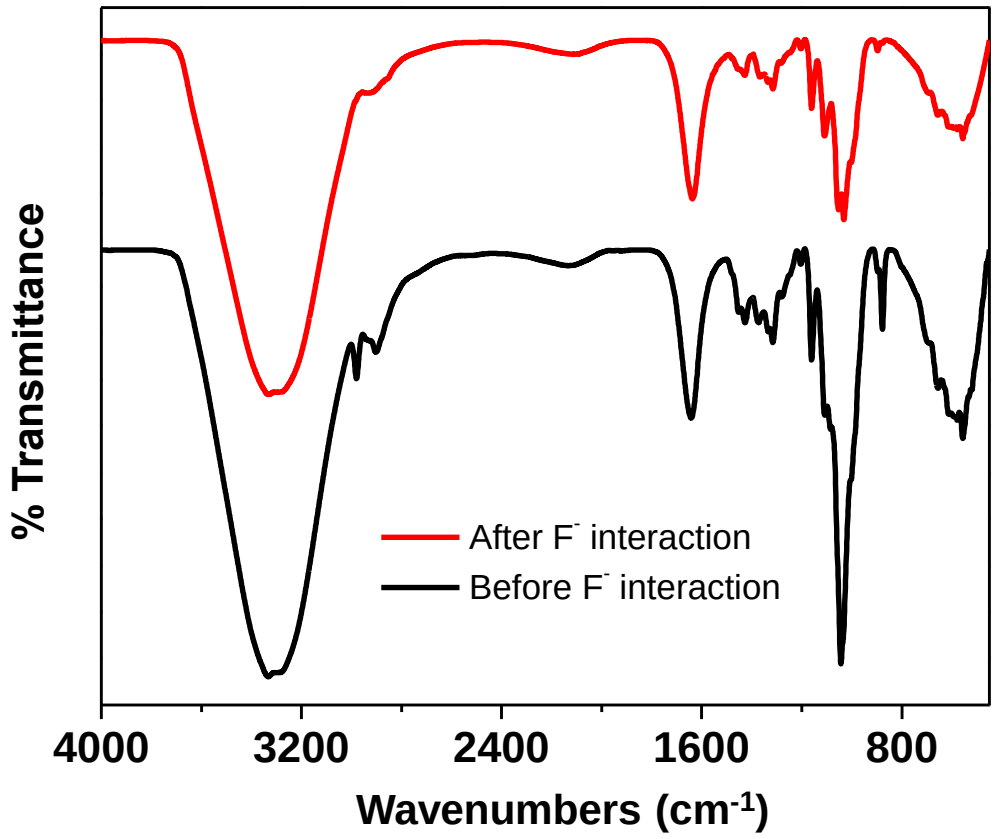

Figure S5. IR spectra showing NC-XO before and after interaction with F^- ions.

The wide band at 3000–3600 cm^{-1} is assigned to O–H vibrations. The sharp bands at ~2948 cm^{-1} are assigned to the asymmetric and symmetric methylene stretching modes. The sharp bands at ~1078 cm^{-1} are assigned to the C–O stretching vibration of alcohol. These characteristic bands can confirm the existence of glycol. The bands at ~1653 cm^{-1} is assigned to the C=O vibrations, which implies that there is partly oxidation of glycol in the reaction process. Slight shifts in the C-O and C=O stretching frequencies to higher wavenumbers is observed upon interaction with F^-.

Supplementary information 6

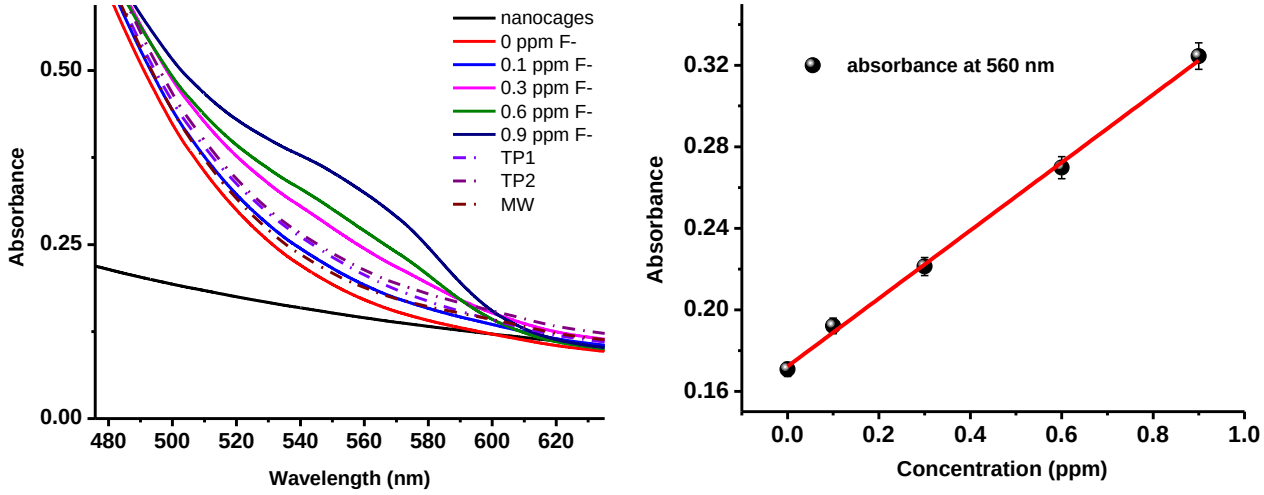

Figure S6. Absorbance spectra showing NC-XO interaction with standard F^- solutions and various commercial dental products (left). Standard curve for F^- content estimation in the dental products (right).

UV-vis spectra show the sensor response with 0, 0.1, 0.3, 0.6 and 0.9 ppm F- standards to make a standard curve, that helped to quantify the F^- content in TP1, TP2 and MW samples by their respective absorbance values.

Supplementary information 7

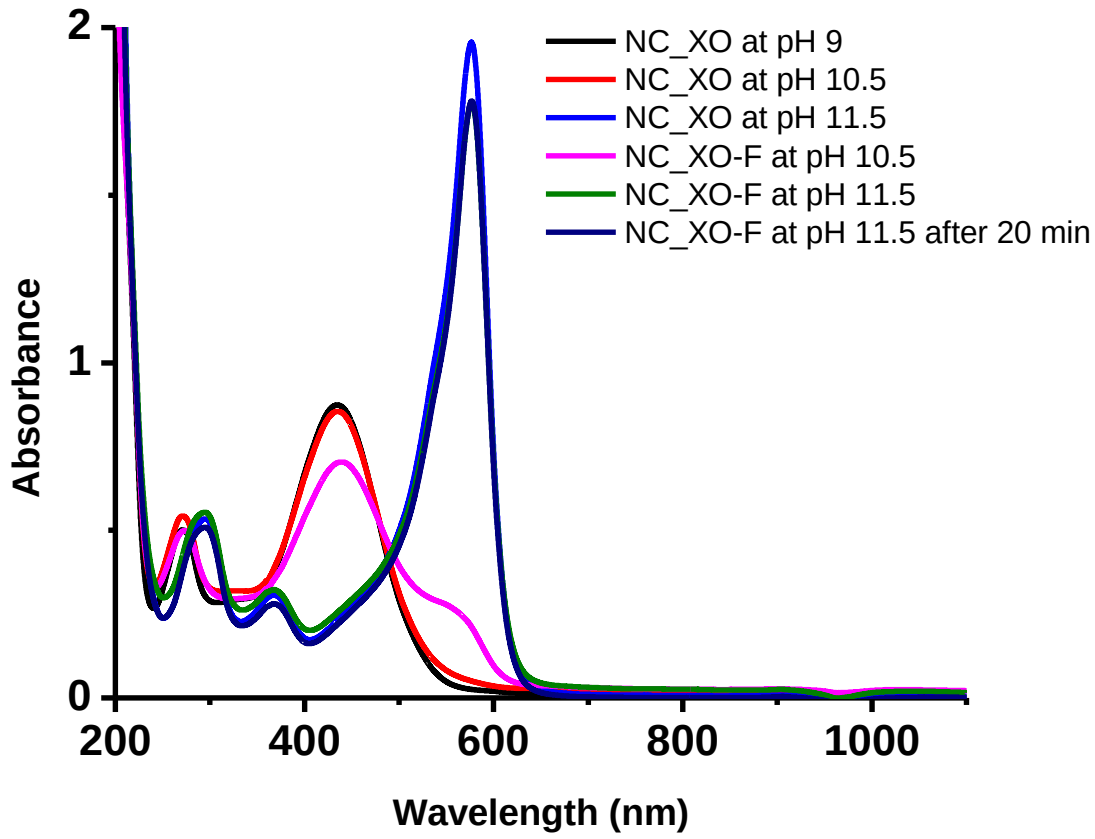

Figure S7. Absorbance spectra of NC-XO before and after F^- interaction, at various alkaline pH conditions.

UV-vis spectra were taken to observe the pH dependent behavior of the sensor. Control studies showed that NC-XO gives consistent results till pH 10.5 in case of with and without F^- samples. At pH 11.5 and beyond, NC-XO undergo color changes without any F^- in the medium.

Supplementary information 8

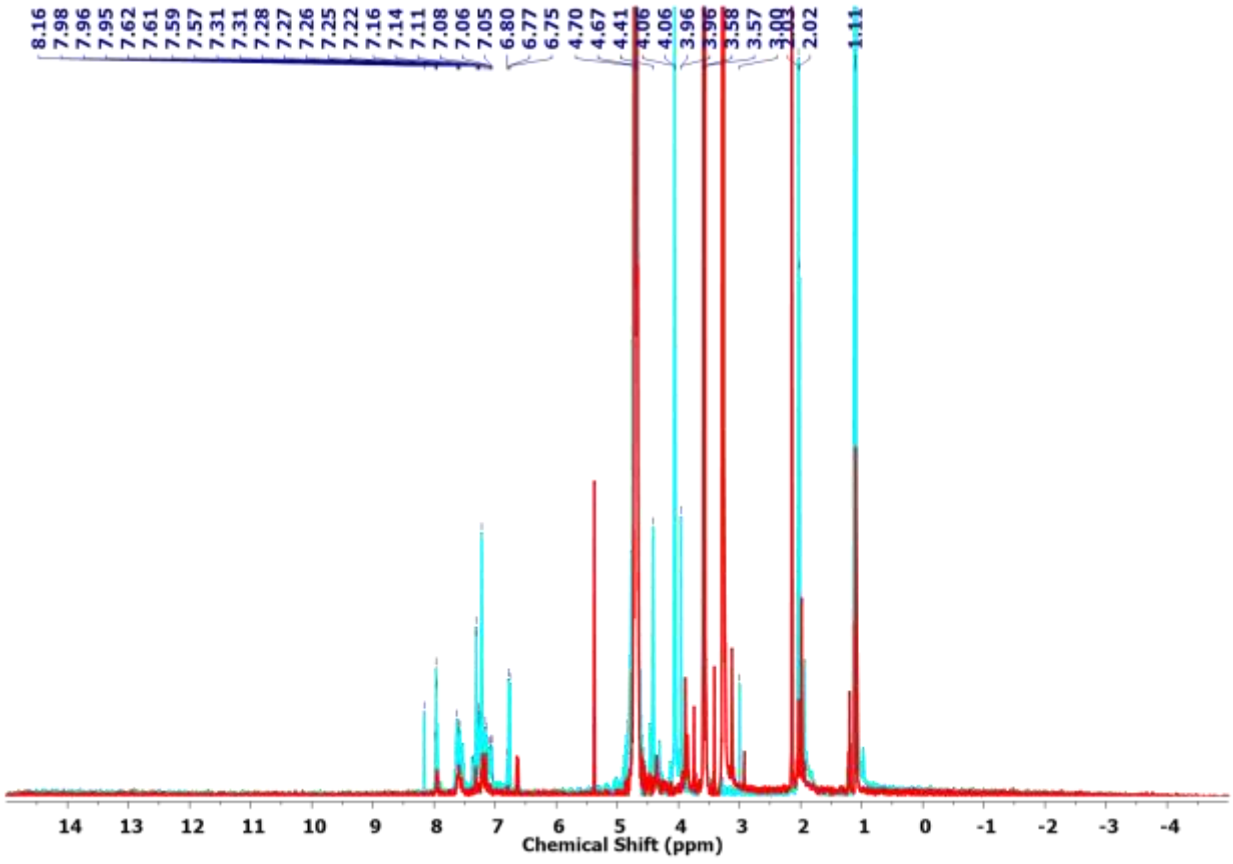

Figure S8. Overlapping full length ^{1}H NMR spectra of XO and NC-XO-F.

XO: 1H NMR {D2O, 500 MHZ, δ} =

2.02, 2.03 (two S, 6H, CH3), 3.96, 4.41 (two S, 12H, CH2), 6.77 (S, 2H, OH), 7.11 (m, 4H, Ph-SO3-), 7.61 (m, 4H, Ph) 7.98 (m, 4H, COOH) 7.3 (m, 6H, benzene)

NC-XO-F: 1H NMR {D2O, 500 MHZ, δ} =

2.03, 2.15 (m, 6H, CH3), 3.13 (S, 2H, NH+), 3.88, 4.35(m, 12H, CH2), 6.62 (d, 1H, OH), 7.22 (m, 4H, Ph-SO3-), 7.59 (m, 4H, Ph), 7.95 (d, 2H, COOH).

Supplementary information 9

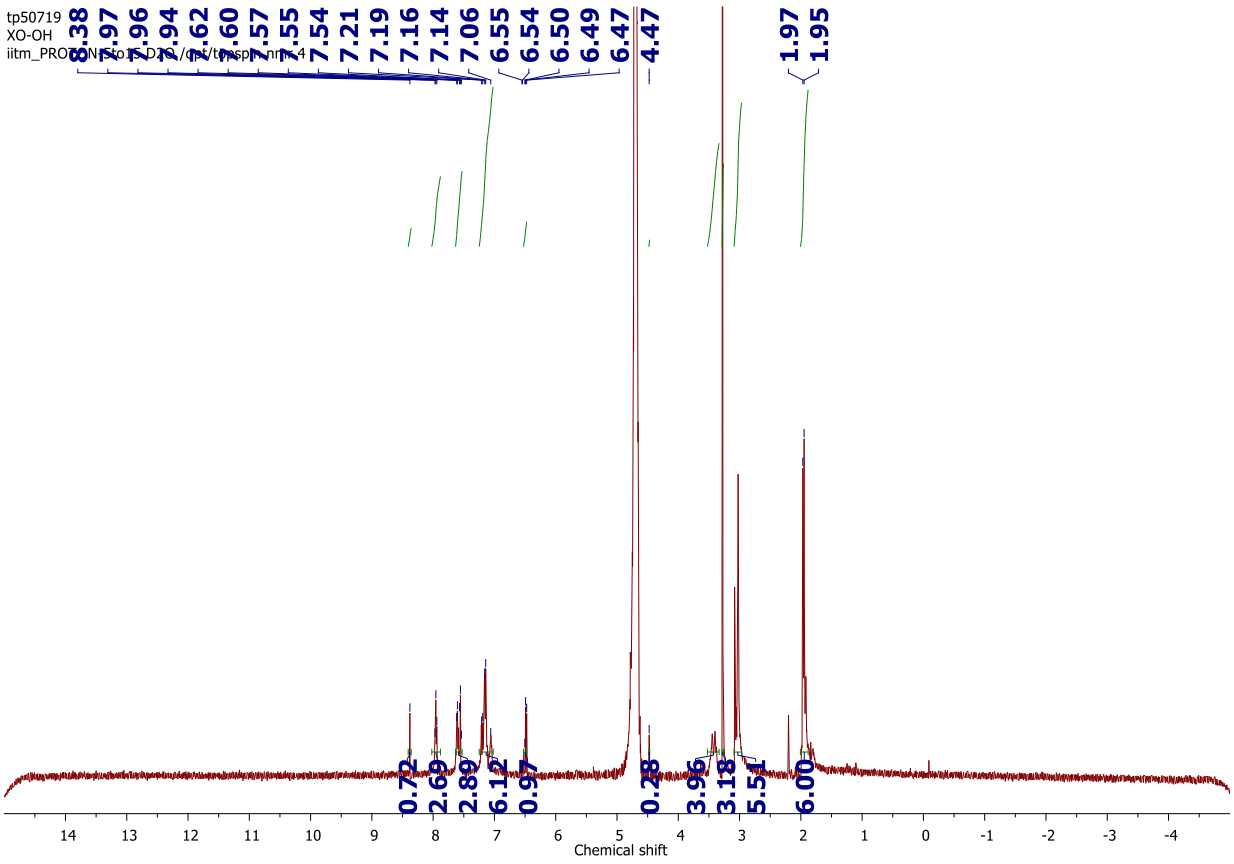

Figure S9. Full length ^{1}H NMR spectrum of XO at pH 11.5.

The NMR peaks of XO at 11.5 and neutral pH (Figure S8) do not match, hence some chemical transformation in the dye structure at very high alkaline pH is evident.

So, working pH for the sensor is from acidic to pH 10.5.

Supplementary information 10

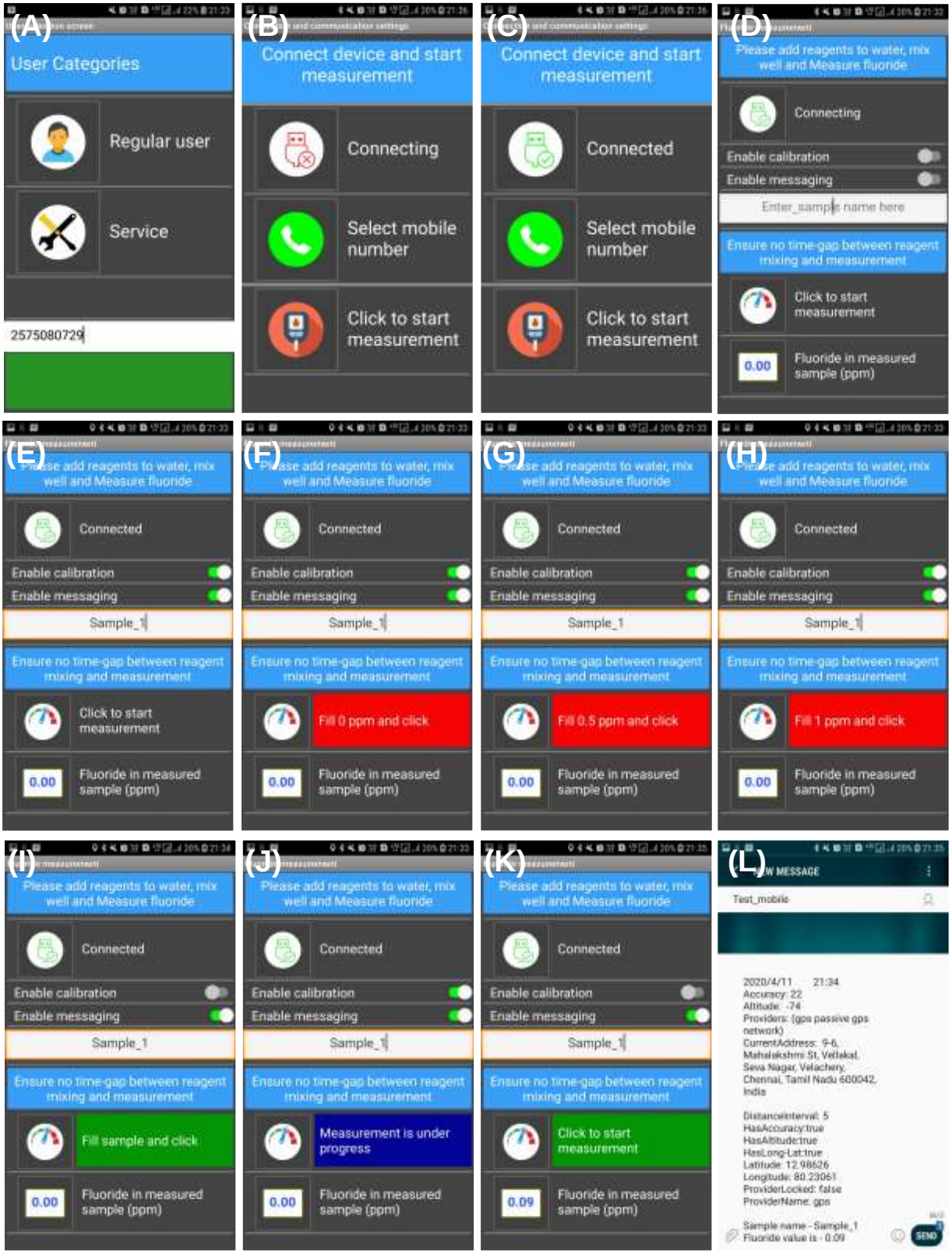

Figure S10. (A) to (L) show steps for using the fluoride sensor app over an android supporting phone for connection, calibration and measurements (output values not to be considered).

Supplementary information 11

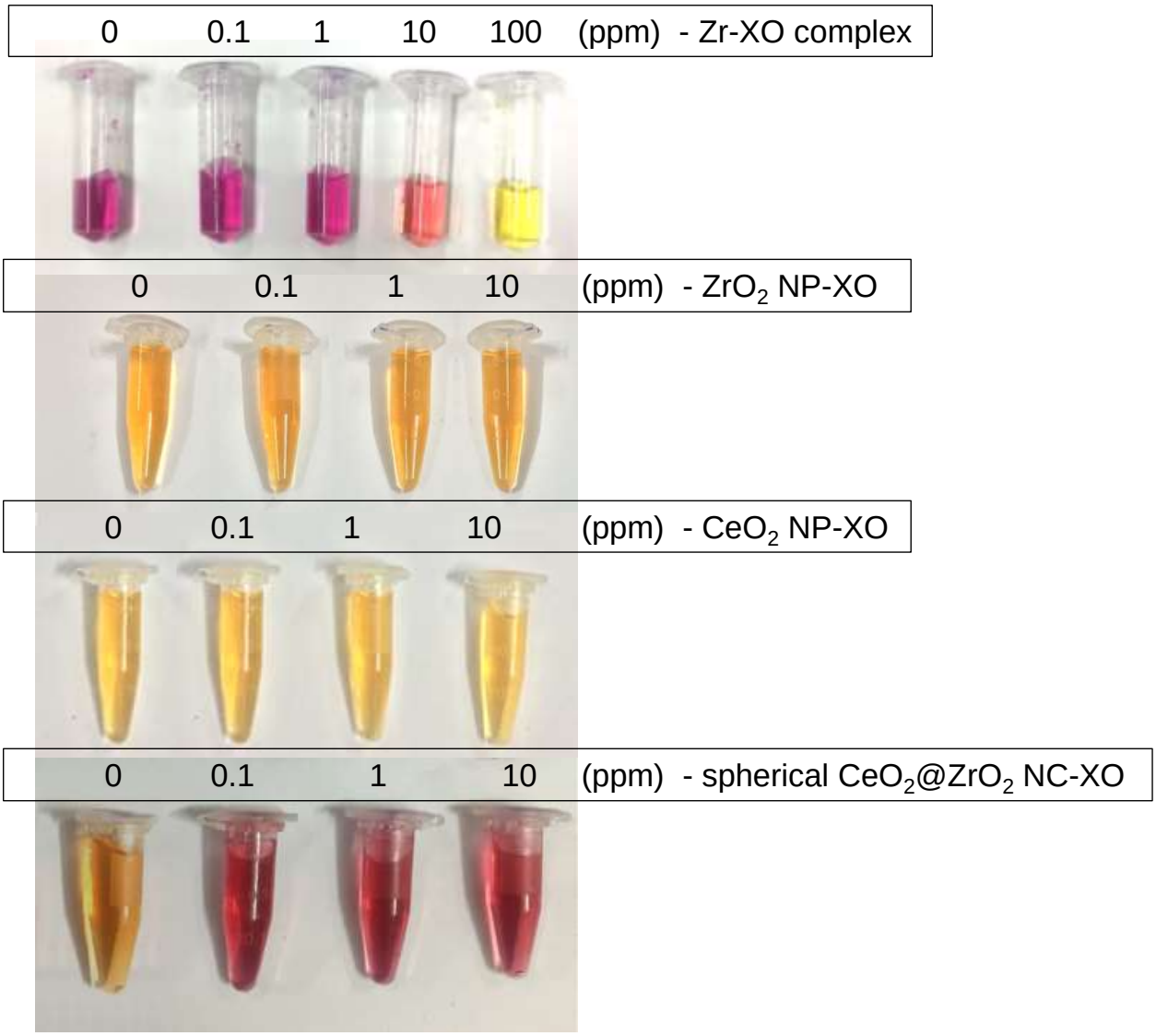

Figure S11. Optical images of control F- sensing experiments performed with zirconium-XO complex, ZrO_2 NP-XO, CeO_2 NP-XO and spherical CeO_2@ZrO_2 NC-XO systems for 0, 0.1, 1 and 10 ppm of F-.